Journal of Fluorescence (2019) 29:693–702
https://doi.org/10.1007/s10895-019-02381-5

ORIGINAL ARTICLE

Optical Recognition of Ammonia and Amine Vapor Using "Turn-on" Fluorescent Chitosan Nanoparticles Imprinted on Cellulose Strips

Tawfik A. Khattab[1] · Nesrine F. Kassem[2] · Abeer M. Adel[2] · Samir Kamel[2]

Received: 4 January 2019 / Accepted: 17 April 2019 / Published online: 30 April 2019

Abstract

A practical fluorescent test dipstick for an efficient recognition of ammonia and amines vapors was developed. The prepared testing strip was based on a composite of molecularly imprinted chitosan nanoparticles, supported on cellulose paper assay, with artificial fluorescent receptor sites for ammonia/amines recognition in aqueous and gaseous phases. A modified chitosan nanoparticles containing fluorescein molecules, were successfully prepared and employed on cellulose paper strip creating fluorescent cellulose (FL-Cell) to act as "turn-on" fluorescent sensor for sensing and determining ammonia and organic amine vapor. We employed chitosan nanoparticles that had fluorescein incorporated as the fluorescent probe molecule, with a readout limit achieved for aqueous ammonia as low as 280 ppm at room temperature and atmospheric pressure. The sensor responded linearly relying on the aqueous ammonia concentration in the range of 0.13–280 ppm. The chromogenic fluorescent cellulose platform response depended on the acid-base characteristic effects of the fluorescein probe. The protonated form of fluorescein molecules immobilized within the chitosan nanoparticles were in a nanoenvironment demonstrating only weak fluorescence. When binding to ammonia/amine vapor, the fluorescein active sites were deprotonated and exhibited higher "turned-on" fluorescence as a result of exposure to those alkaline species. The simple fabrication and abovementioned characteristics of such fluorescent chitosan nanoparticles are such that they should be applicable for monitoring of ammonia/amines in either aqueous or vapor states. We studied the distribution of the fluorescent chitosan onto paper sheets fabricated from bleached bagasse pulp and coated with two different thicknesses of a fluorescent nanochitosan and blank nanochitosan solutions. A thin fluorescent nanochitosan layer was created on the surface of cellulose strips using an applicator. Its distribution was assessed by scanning electron microscopic (SEM) and transmission electron microscopic (TEM) analysis as well as Fourier-transform infrared spectroscopic (*FT-IR*) measurements. The mechanical properties were also tested. The exploitation of this "turn-on" fluorescence sensor invented platform should be amenable to different situations where determination of ammonia/amine vapor or aqueous solution is required.

Keywords Chitosan · Nanoparticle · Molecular imprinting · Ammonia · Amine · Fluorescent sensor

Introduction

Ammonia and organic amines represent a very important category of organic chemicals that have been used in various fields, such as pharmaceutics, agriculture, foodstuff industries, cosmetics, and automotives [1–3]. As a result of their high toxicity, the development of fast recognition testing techniques for ammonia/amines in either aqueous or gaseous phases is of high significance for environmental monitoring purposes and *quality assurance*. Detecting ammonia is also significant for a number of clinical illness diagnostic applications [4–8]. Natural polymeric materials, such as cellulose, chitin and starch, comprise essential renewable resources of inventive functional materials, which present a substitute in response to the economical and depletion problems accompanied to utilizing fossil counterpart [9, 10]. Recently, chitosan, the deacetylated product derived from chitin, has particularly attracted a great interest due to its remarkable characteristics, including biocompatibility and bioactivity, which make it mainly suitable in a variety of applications, such as

✉ Tawfik A. Khattab
ta.khattab@nrc.sci.eg

[1] Dyeing, Printing and Auxiliaries Department, National Research Centre, Cairo 12622, Egypt

[2] Cellulose and Paper Department, National Research Centre, Cairo 12622, Egypt

agriculture, biomedical, pH sensitive drug delivery, and ecological protection purposes [11, 12]. Chitosan is characterized by its hydrophilic nature and the availability of a great number of amino and hydroxyl substituents to act as active sites applicable for various interesting chemical amendments. The application of chitosan as a coat on a paper surface or as an additive in papermaking has been explored to demonstrate an excellent ability of chitosan to generate strong thin layers, accordingly enhancing the properties of the ensuing coated substrates, such as mechanical performance and antimicrobial activity [13–17]. Biomolecules have been labeled by fluorescent sites for determining certain analytes. Fluorescent chitosan have been employed in some biologically associated applications, however, to the best of our knowledge, they were never described as a sensor additive to cellulose paper strips. Organic fluorescent fluorophores have been broadly employed in bioimaging and medical diagnostic purposes; nonetheless they have considerable limitations, such as low intensity of spectrum band, photobleaching and broad fluorescence emission spectrum, which could be simply interfered by a background fluorescence emission band produced by the sample matrix [18–22].

Optical probes have been used for detecting and determining ammonia and amine compounds. They usually present cheap platforms that can be practically and simply fabricated into various miniaturized structures, such as thin films, nanofibers and nanoparticles; meanwhile introduce high quality in terms of sensitivity and selectivity. The sensor platform major component is typically an absorption or emission generating probe species whose band intensity varies when exposed to the detected analyte [23, 24]. Optical sensor devices based on sensor molecular fluorophores allow for qualitative and quantitative discrimination of organic analytes, such as ammonia and organic amines. Fluorescence-based probes display either a reduction "turn off" of the emission band due to quenching or an enhanced "turn on" of the fluorescence spectrum band. The "turn-on" type probes are favored due to their higher sensitivity and selectivity, compared to "turn off" category of probes [25, 26]. Fluorescein, particularly, has been used as a probe in the fabrication of a fluorescent sensing platform due to its high quantum yield. Furthermore, its excitation and emission wavelengths are located in the visible spectrum, which is valuable for its detection process. Fluorescein fluorophore has been employed for a variety of applications, such as pH sensor, tracer in proteins labeling, cosmetics, determining the structure of cells, as a laser dye and for forensic purposes [27–29].

There are different analytical techniques have been applied for detecting ammonia/amines, such as specific ion membrane electrode, UV-visible absorption spectrophotometry and titrimetric analysis. Those analytical techniques have been applied for both aqueous and liquid amine comprising samples; however they are not applicable for gaseous state analytes or continuous monitoring purposes. Many electrochemical recognition tools have also been recognized depending on the reaction of the amine with the sensing material, such as polypyrrole-platinum nanocomposite and metal oxide-based semiconductor. However, such electrochemical sensors are irreversible, slow, and/or necessitate high processing temperatures [30–36].

In this paper, we describe the invention of a highly sensitive "turn-on" fluorescent cellulose strips loaded by fluorescent sensor that is comprised from the preparation of fluorescent chitosan nanoparticles onto which fluorescein probe molecules were chemically bonded. The fluorescein active sites within the chitosan nanoparticle medium exhibit only very weakly emission spectrum; nonetheless, when exposed to ammonia/amine vapor or aqueous medium, the fluorescein active sites becomes deprotonated leading to an improved fluorescence intensity spectrum band. The fabrication of the fluorescent cellulose platform and its characteristics, analytical performance and mechanical properties, responding time, reusability, sensitivity, and selectivity were described.

Experimental

Materials and Reagents

Kraft bagasse was obtained from Edfu Sugar and Paper Pulp Mills, Egypt. The bleaching process of Kraft bagasse pulp was performed using chlorine dioxide. Chemical analysis was performed to determine the percentage of the main chemical constituents of the bleached Kraft bagasse pulp to display Klason lignin (1.05%), α-cellulose (73.32%), hemicelluloses (19.68%), and ash contents (0.32%). Fluorescein isothiocyanate ($C_{21}H_{11}NO_5S$), Mw. 389.38, was supplied from Mallinckrodt Inc. Chitosan commercial grade (Oxford Laboratory, India) with 90–95% degree of deacetylation, was used.

Methodology

Bleaching

The pulp was bleached using sodium hypochlorite one-step procedure. The bleaching requirement was 4 g of chlorine per 100 g of the sample at pH 7–9, consistency 5% at 80 °C for 1.5 h with occasional shaking, after which the pulp was washed till neutrality.

Paper Manufacture

The paper sheets were prepared according to the S.C.A standard, using the model S.C.A sheet former (AB Worentzen and Wettre). In the apparatus a sheet of 165 mm diameter and 214 cm^2 surface area was formed. The weight of oven dry

pulp used for every sheet was about 1.8 g. After sheet formation, the sheet was pressed for 4 min using a hydraulic press. Drying of the test sheets was made with the help of a rotating cylinder or drum.

Synthesis of Nanochitosan and Fluorescent Nanochitosan

0.5 g of chitosan was dissolved in 100 ml of 1% (*v*/v) acetic acid solution. 1 ml of an aqueous solution of sodium tripolyphosphate (0.25% *w*/*v*) was added into the chitosan solution under magnetic stirring for 2 h at ambient temperature. The chitosan nanoparticles could be centrifuged at 16000 rpm and then rinsed with distilled water and air dried.

The fluorescent nanochitosan was prepared by the reaction of the amino group of nanochitosan with the isothiocyanate group of fluorescein fluorophore. 0.5 mg/ml solution of fluorescein isothiocyanate in methanol was slowly added under continuous stirring to a 1% *w*/*v* solution of the purified nanochitosan in 1% *v*/v aqueous acetic acid. The condensation interaction between the isothiocyanate functional substituent of the fluorescein isothiocyanate fluorophore and the amino functional substituent of nanochitosan was allowed to proceed in the dark and at ambient temperature, followed by addition of 10% NaOH aqueous solution to afford a solid powder.

Coating of Paper Sheets

The bleached kraft bagasse paper sheets were coated with 2% nanochitosan or fluorescein- nanochitosan solutions in 1% *v*/v acetic acid using an applicator. Coating of paper sheets were applied using 60 and 120 μm thickness layers using doctor blade film applicator. The coated paper sheets were dried at 100 °C.

Sensor Testing

To test the fluorescent cellulose sensor for detection of ammonia vapor, an aqueous ammonium hydroxide solution (5 ml) was placed in a 10 mL test tube. The fluorescent cellulose sample was placed near the top of the test tube demonstrating an immediate change in fluorescent intensity due to exposure to the generated ammonia gas at room temperature and atmospheric pressure. The reversibility was monitored by observing λ_{max} at the fluorescence emission maximum at 509 nm (absorption values are 70 and 444 in absence and presence of ammonia vapor, respectively) for the fluorescent cellulose at ambient temperature. The emission spectra were switched back and forth between 410 and 525 nm in absence and presence of ammonia gas and the emission maxima were recorded for each cycle.

Analyses and Characterizations

Mechanical Properties

The treated and untreated paper samples were conditioned for 24 h in a standard atmosphere (at 23 °C and 50% relative humidity), prior to testing for tensile strength and burst. Tensile testing was carried out on 15 mm wide strips between jaws set 100 mm apart, using a LLOYD LR 10 K universal testing machine. For burst, a Mullen tester (Perkin, Chicopee, Mass, USA) was used.

Infrared Spectrophotometer

Fourier transform infrared (FTIR) spectra of blank nanochitosan and fluorescein-functionalized nanochitosan were recorded by using KBr disc technique in the range of 400–4000 cm^2 on Shimadzu 8400S FT-IR Spectrophotometer.

Transmission Electron Microscopy

Nanochitosan was characterized by TEM using a JEOL 1230 transmission electron microscope (JEOL, Tokyo, Japan) with acceleration voltage of 100 KV. A drop of nanofiber suspension was used on a copper grid bearing a carbon film.

Scanning Electron Microscopy

Scanning electron microscopy (gold coating, Edwards Sputter Coater, UK) was performed using a Jeol 6310 (Jeol Instruments, Tokyo, Japan) system running at 5–10 kV.

Fluorescence Study

Fluorescence emission and excitation spectra were recorded by JASCO spectrofluorometer FP-8300 providing corrected excitation spectra directly. The emission spectra were reported by excitation at the corresponding absorption maxima (490 nm), and the excitation spectra were reported at the corresponding emission maxima (519 nm).

Results and Discussion

Synthesis of Fluorescent Chitosan

The previously bleached kraft bagasse paper sheets were coated by either 2% nanochitosan or fluorescent nanochitosan dispersed in 1% *v*/v acetic acid using an applicator. Coating of paper sheets were applied using 60 & 120 μm thickness layers affording a molecularly imprinted cellulose strips by fluorescein generation of tailor-made binding fluorescein-

based recognition sites on the nanochitosan polymer chains (Scheme 1). These fluorescein-based detection sites are able to specially capture ammonia and amines in both vapor and aqueous phases. Thus, it seems to be of great significance to employ molecularly imprinted cellulose polymer to determine selectively the trace-level of ammonia and amines which exist in low concentrations or in a complex matrix.

Morphological Properties and Elemental Analysis

Solid-state sensor materials are characterized by simplicity, portability and reversibility, which lead to fast online detection achievable at low price. Solid-state sensors are even more practical than liquid probes [2]. Therefore, it is very interesting and also challenging, to fabricate solid-state sensing materials for real-time recognition of a trace target substance in either solution or vapor state. A solid detector could eventually be used as simple portable devices for essential laboratory assays and for household applications as commercial detectors. Thus, the drilling for an eco-friendly simple solid-state detector is of great importance. Cellulose is one of the highly significant natural biopolymers [7]. Chitosan nanoparticles are generally solid multifunctional materials with a porous network, which is characterized by high surface area, high mechanical and thermal insulation, high porosity, and low density [37, 38].

The morphological properties of the coated paper sheets were evaluated. As was obvious in the scanning electron microscope (SEM) images (Fig. 1), the surface of the fluorescent cellulose platform was successfully coated by a thin layer of fluorescent nanochitosan. Visually, surface seems to be homogeneous with regular distribution of the coat on the surface which indicates strong hydrogen bonding between components. Moreover, the SEM images illustrated no variation was monitored in the paper surface platform after coating by nanochitosan only without the fluorescent dye. On the other hand, the transmission electron microscope (TEM) images (Fig. 2) displayed the size distribution of the fluorescent chitosan nanoparticles ranging between 5 and 20 nm scale. It was observed that the nanochitosan film tended to aggregate, and hence dispersed slightly homogeneously onto the paper sheet surface. This could be ascribed to the type of chemical reaction between the fluorescent nanochitosan polymer chains and the paper sheet surface.

In order to investigate the existence of chitosan component and its attachment mechanism to cellulose strips, FT-IR spectroscopy is the most important tool. Structural characterization of chitosan, nanochitosan and fluorescent nanochitosan; are demonstrated in Fig. 3. Chitosan comprises various hydroxyl and secondary amine substituents on the repetitive glucose polymer chain units. This was proved by the absorption at 3300 cm^{-1}, pointing to the stretching vibrations of the amino and hydroxyl groups, which displayed a clear shift to higher wavenumber value (3427 cm^{-1}) in the fluorescein-functionalized nanochitosan to verify that fluorescein moiety was introduced into chitosan polymer chains. An absorption band was monitored at 2921 cm^{-1} which can be assigned to

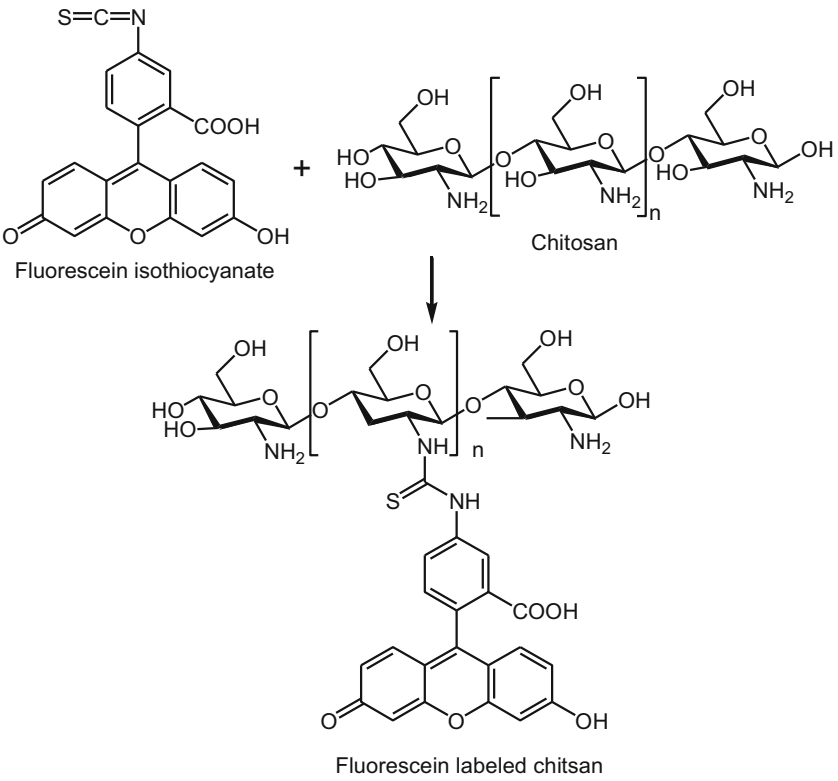

Scheme 1 Synthesis of fluorescein-labeled nanochitosan

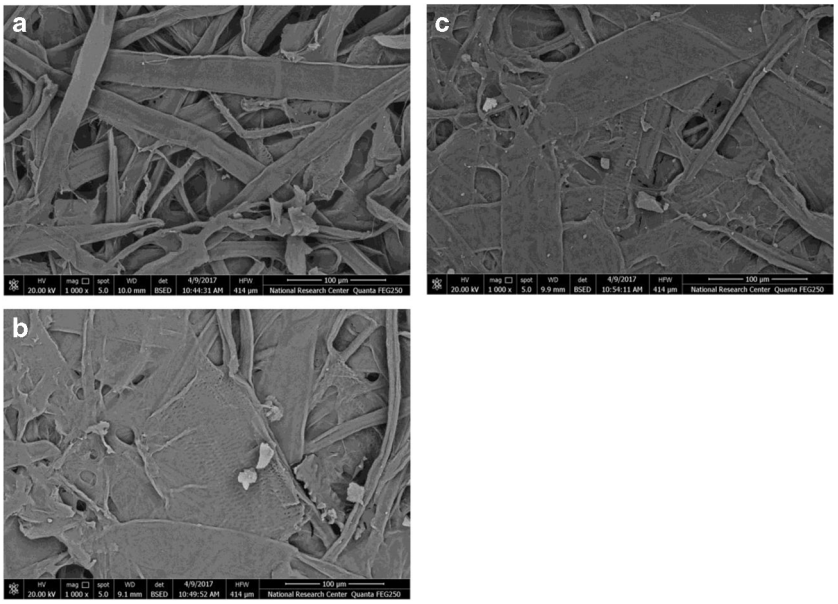

Fig. 1 SEM images of uncoated paper sheets (**a**), paper sheets coated with nanochitosan (**b**) and paper sheets coated with fluorescent nanochitosan (**c**)

aliphatic CH and CH_2. The band at 1073 cm^{-1} was attributed to C-N stretch of the secondary amine. Upon the application of the fluorescent nanochitosan by coating on the cellulosic paper sheet, certain strong bonding could be produced. There were no bands appeared for the fluorescent nanochitosan. Nonetheless, the band intensity of the hydroxyl group at 3300 cm^{-1} was highly decreased as a result of the possibility of ester bond creation between chitosan amino substituent and cellulose hydroxyl substituent.

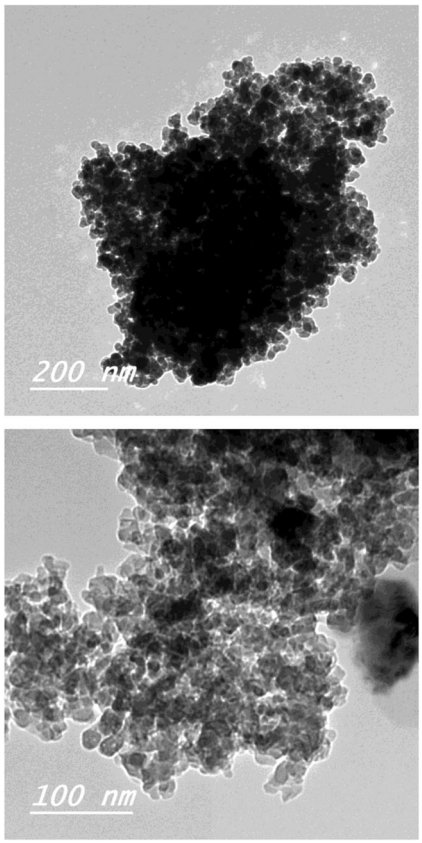

Fig. 2 TEM images of fluorescent nanochitosan

Mechanical Properties

Table 1 represents the mechanical properties of paper sheets before and after coating with different mixtures. This table includes retention, tensile strength and burst factor.

Retention

From Table 1 it can be seen that retention of paper sheets increased by increasing the thickness of coating from 60 to

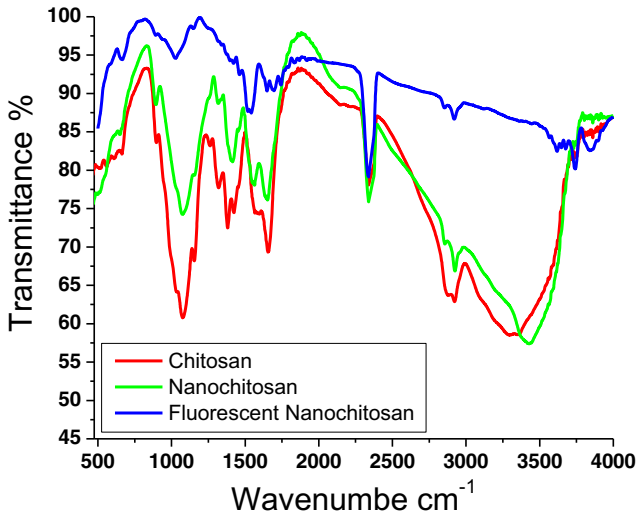

Fig. 3 FT-IR spectra of chitosan, nanochitosan and fluorescent nanochitosan

Table 1 Mechanical Properties of uncoated and coated paper sheets

Sample	Increase in wt. (g/m^2)	Breaking Length (km)	Burst factor
Blank	0	2.3	9.6
Chitosan (60)	140	2.5	11.8
Chitosan (120)	166.7	3.1	12.1
Fluorescent Chitosan (60)	173.3	3.2	12.0
Fluorescent Chitosan (120)	233.3	3.3	16.4
Nanochitosan (60)	260	2.6	11.7
Nanochitosan (120)	273.3	3	15.7
Fluorescent Nanochitosan (60)	360	3.7	27.4
Fluorescent Nanochitosan (120)	366.7	3.8	32.9

120 μ. It can be noticed that the retention of nanochitosan was higher than that of chitosan by about 85% increase, may be because of the nano size of chitosan which can easily penetrates through cellulose fibres. Also, it was found that paper sheets highly retained the coating containing fluorescent either chitosan or nanochitosan, but the retention of fluorescent nanochitosan was higher.

Tensile Strength and Burst Factor

Breaking length of uncoated and coated paper sheets was plotted in Table 1. It can be seen that coating the bagasse paper sheets ameliorated the tensile strength of all samples. Addition of fluorescent slightly increased the breaking length. It was found that the trend of burst factor is similar to breaking length. It can be concluded that there is an improvement in mechanical properties by coating paper sheets with all previously mentioned solutions.

Fluorescent Properties of FL-Cell Solid-State Sensor

Both of fluorescent nanochitosan dispersed in distilled water and FL-Cell paper sensor was subjected to ammonia (or amine) aqueous medium and vapor, respectively. Accordingly, the fluorescence band of the fluorescein active sites was instantly and considerably increased (Table 2; Figs. 4, 5, 6). This improved emission band was a result of increasing the fraction of the fluorescein active sites that were converted from the weakly fluorescent protonated form to its highly fluorescent deprotonated form upon exposure to alkaline aqueous ammonia or its vapor state. In general, it was significant to report that the existence of some moisture, already available in the atmosphere, within the fluorescein-imprinted nanoparticles on cellulose dipstick, was required in order to monitor the sensor responsiveness. This moisture was capable to react with ammonia/amine within the highly porous nanoparticles film to create negatively hydroxide ions facilitating the deprotonation of the fluorescein molecule [36].

Table 2 Fluorescence emission intensity of fluorescent nanochitosan dispersed in distilled water upon increasing ammonia concentration from 0.13 to 280 ppm

Conc. of aqueous ammonia (ppm)	Emission intensity value	λ_{max} (nm)
418	2893	524
356	2897	523
317	2891	524
280	2884	524
219	2349	521
123	2024	520
46	1589	518
0.13	1201	519
0.08	134	519
0.01	127	518
Blank	122	519

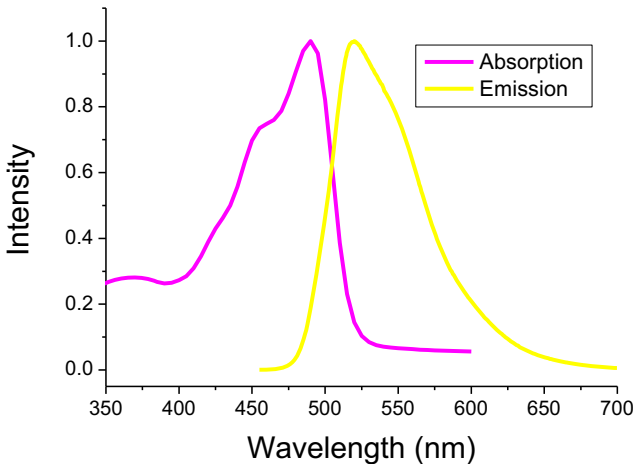

Fig. 4 Normalized excitation and fluorescence emission spectra of fluorescent nanochitosan dispersed in distilled water. The emission spectrum was generated by an aqueous 28% NH_3 solution (excitation and emission wavelengths were 490 nm and 519 nm, respectively)

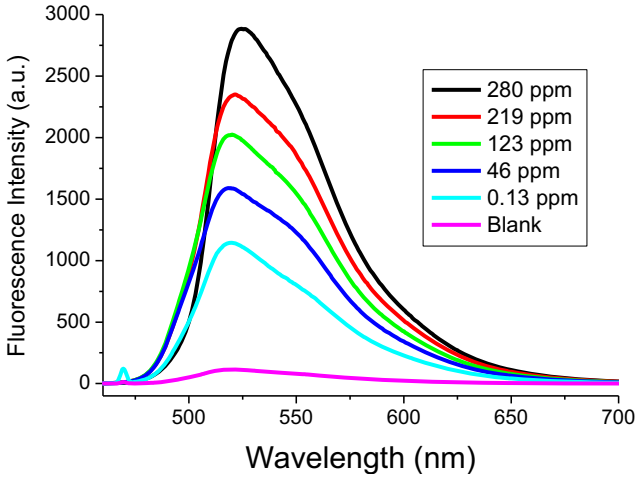

Fig. 5 Fluorescence emission spectra of fluorescent nanochitosan dispersed in distilled water upon increasing ammonia concentration

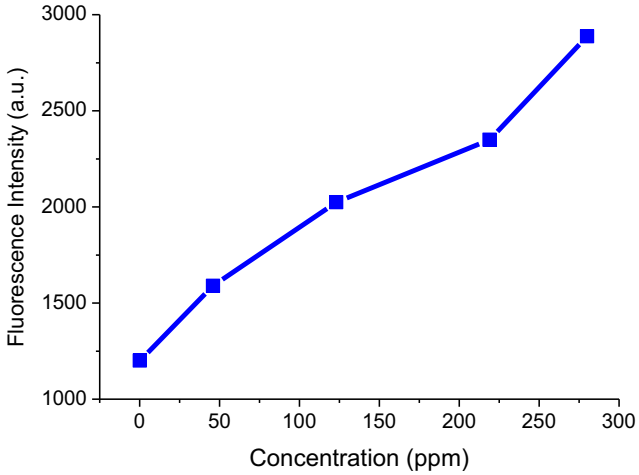

Fig. 7 Fluorescence emission intensity of fluorescent nanochitosan dispersed in distilled water upon increasing ammonia concentration from 0.13 to 280 ppm

The analytical performance of FL-Cell sensor displayed the fluorescence emission spectra obtained upon exposure to ammonia vapor as a function of ammonia concentration. The emission band intensity was found to increase upon increasing ammonia concentration in aqueous phase and the emission band wavelength displayed a small shift to higher wavelength from ~518 to 524 nm. Figure 5 demonstrates the fluorescence spectra of the fluorescent chitosan nanoparticles dispersed in distilled water (15 mL) upon increasing ammonia concentration from 0.13 to 280 ppm by the gradual addition of an aqueous solution of ammonium hydroxide (28% NH_3 in H_2O, ≥ 99.99%).

Figure 7 displays the plotted relationship of the intensity of emission spectra versus the ammonia concentration between 0.01 and 418 ppm. As was apparent, the emission intensity was found to increase when the aqueous ammonia concentration is higher than ~0.13 ppm demonstrating a linear relationship with increasing the concentration of ammonia over the range of 0.13-280 ppm. The FL-Cell sensor platform also responded to only aliphatic amine vapors. The presence of amines in solution affects the pH of the medium. A wide variety of amines with different pK_b values (Table 3) including aromatic and aliphatic (primary, secondary, tertiary) amines. The type of amine used did not significantly influence the essential optical properties of the deprotonated fluorescein form. Generally, the fluorescence emission spectra were almost compatible with the amines pK_b values because the FL-Cell sensor strip showed higher sensitivity for the aliphatic amines, while no sensitivity were detected for the aromatic amines. Less basic aromatic and heterocyclic amines such as aniline and pyridine proved more difficult to detect. Distinct selectivity was also observed along different aliphatic amines, parallel to the basicity of each amine. For aliphatic amines, the selectivity order of the fluorescence improvement followed the sequence: secondary > primary > tertiary amines as shown in Fig. 8. No variations in the fluorescence band was monitored upon exposure to the vapors of different solvents, such as acetone, chloroform, dichloromethane, dimethyl sulfoxide, glacial acetic acid, tetrahydrofuran, ethanol, dimethylformamide, *n*-hexane, methanol and toluene. These organic reagents and substances did not display any interference in the sensor performance.

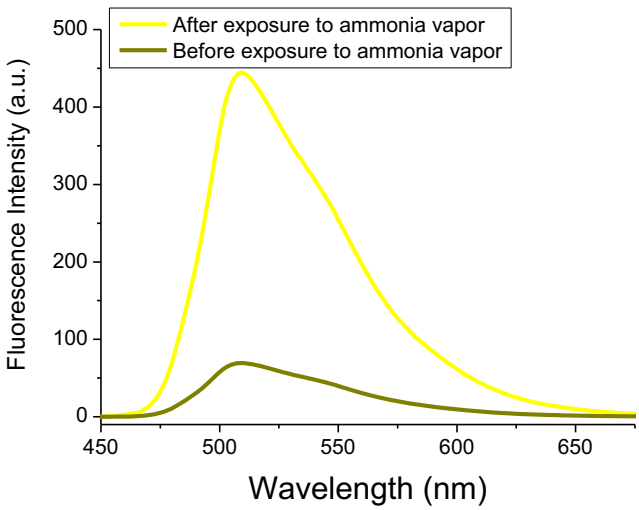

Fig. 6 Changes in fluorescence emission spectra of fluorescent cellulose dipstick (FL-Cell) at 509 nm before and after exposure to ammonia vapor (excitation at 490 nm)

The response time was very fast (less than a second) for FL-Cell platform; even at the very low concentration of ammonia gas. This fast responsiveness can apparently be attributed to the porous three-dimensional nanoparticles this layer that permits fast diffusion and flow of the ammonia gas into the chitosan nanoparticles matrix where it can then react with the fluorescein active molecular sites. The time period needed for the sensor platform recovery and the return of the strong

Table 3 Changes in fluorescence intensity value (at 509 nm) of FL-Cell against different types of amines in vapor state

Amine number	Amine name	Amine category	Fluorescence intensity	pK_b value* [39–43]
1	Tributylamine	Tertiary aliphatic	795	3.11
2	Triethylamine	Tertiary aliphatic	880	3.25
3	Diethylamine	Secondary aliphatic	1517	3.16
4	Piperidine	Secondary aliphatic	1683	2.89
5	*n*-Butylamine	Primary aliphatic	1275	3.40
6	Ethylamine	Primary aliphatic	1123	3.35
7	Pyridine	Aromatic	107	8.77
8	Aniline	Aromatic	80	9.13

*Base Ionization Constants in Water at 25 °C

fluorescent spectrum band back to its pristine weak value was ~5 min under atmospheric conditions. To examine the reversibility of this FL-Cell sensor, the emission wavelength was switched back and forth among the two emission intensity values 70 (in absence of ammonia vapor) and 444 (in presence of ammonia vapor) at wavelength 509 nm, while reporting the emission intensity value for each cycle. The ratios of fluorescence intensities at 509 nm were recorded. The emission spectrum band, once recovered, displayed the same emission improvement responsiveness when re-exposed to ammonia gas following to every recovery cycle. Figure 9 displays continuous cycles of the emission improvement recovery-responsiveness cycle following to exposure to ammonia gas and showed that the spectrum band variations were highly reversible. Efficient and reversible fluorescent emission responses without fatigue were monitored for this FL-Cell sensor platform after repetitive use, proving high stability.

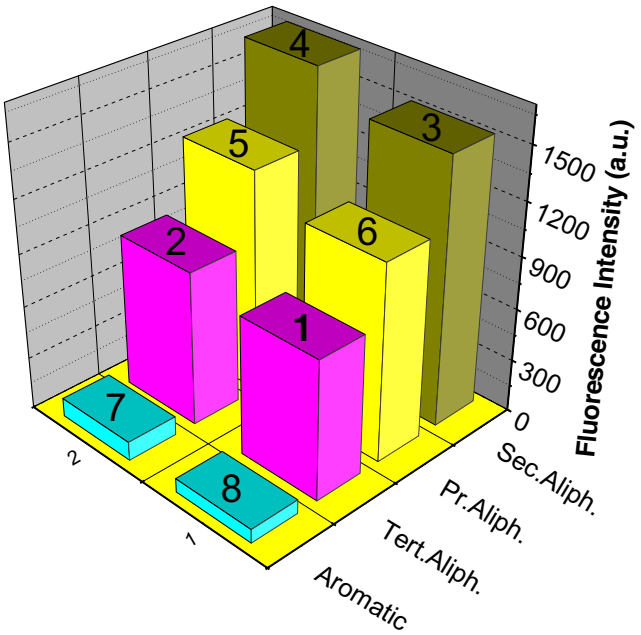

Fig. 8 Changes in fluorescence intensity (at 509 nm) for different types of amines in vapor state

Proposed Mechanism of FL-Cell Sensor

Ammonia/amines were determined by taking benefit of the acid/base related fluorescence effects of the fluorescein fluorophore molecules that were chemically bonded to the chitosan nanoparticles. The ammonia/amine vapor diffuses and flows into and within the nanoparticle matrix loaded on the cellulose strips causing deprotonation of the fluorescent probe active sites (Scheme 2). The fluorescence of the FL-Cell was improved because the fluorescence quantum efficiency of the deprotonated fluorescein was higher than that of the protonated fluorescein fluorophore. Therefore, the fluorescent chitosan nanoparticles acts as a "turn-on" signal creator. Upon the removal of the FL-Cell strip away from the analyte vapor source, the fluorescent nanoparticles, comprising high surface area and high porosity, assisted the diffusion of the ammonia/amine vapor out of the fluorescent nanoparticles thin layer with simultaneous reprotonation of the fluorescein active sites. [44–47].

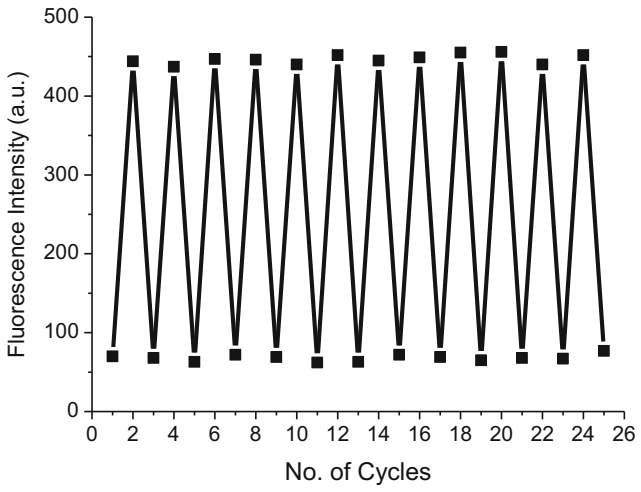

Fig. 9 Changes in the ratio of fluorescence intensity at 509 nm of FL-Cell sensor in absence (fluorescence intensity was 70) and presence (fluorescence intensity was 444) of ammonia vapor at ambient temperature and atmospheric pressure

Scheme 2 Sensing mechanism of the fluorescein active sites imprinted on nanochitosan

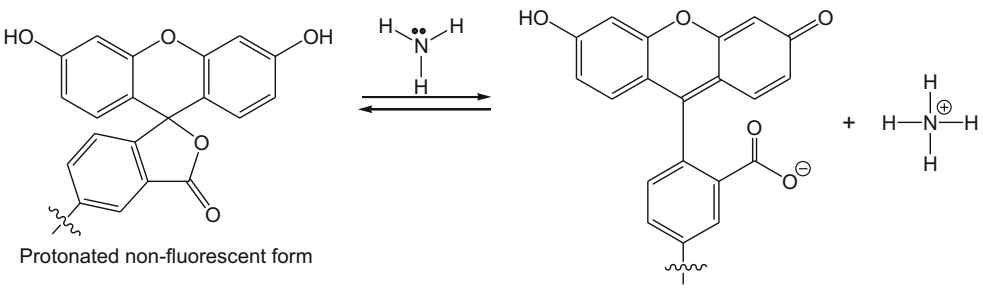

Protonated non-fluorescent form

Deprotonated fluorescent form

Conclusion

A novel cellulose "turn-on" fluorescence signal platform was developed by coating a thin layer of fluorescent chitosan nanoparticles on cellulose substrate for selective detection of ammonia/amine vapor. The fabricated "turn-on" fluorescence sensor with high surface area and high porosity of the chitosan nanoparticles allowed for the inclusion of fluorescein active sites by chemical bonding. The simple fabrication of this fluorescent cellulose platform along with its fast detection, reversibility, high sensitivity and operational simplicity make it potentially typical for discrimination of ammonia/amine vapor in a wide range of fields. The FL-Cell responded selectively to aliphatic amines vapors with the relative fluorescent spectrum band responsiveness following the sequence: secondary > primary > tertiary amines. No signal was detected for aromatic amines. Its distribution was assessed by scanning electron microscope and transmission electron microscope observations as well as Fourier-transform infrared spectroscopic measurements. The results demonstrated a highly homogeneous surface distribution and that the retention of coating solution within the paper pores increased. As compared to the conventional detection techniques of ammonia and amines, the developed testing platform was characterized by small size, operational simplicity, portability and cheapness.

Acknowledgements The authors sincerely acknowledge the National Research Center of Egypt for financial support of this research activity under grant number 11090110.

Compliance with Ethical Standards

Conflict of Interest None.

References

1. Stratton JE, Hutkins RW, Taylor SL (1991) Biogenic amines in cheese and other fermented foods: a review. J Food Prot 54(6): 460–470
2. Khattab TA, Rehan M, Aly SA, Hamouda T, Haggag KM, Klapotke TM (2017) Fabrication of PAN-TCF-hydrazone nanofibers by solution blowing spinning technique: naked-eye colorimetric sensor. J Environ Chem Eng 5(3):2515–2523
3. Onal A (2007) A review: current analytical methods for the determination of biogenic amines in foods. Food Chem 103(4):1475–1486
4. Khattab TA, Tiu BDB, Adas S, Bunge SD, Advincula RC (2016) Solvatochromic, thermochromic and pH-sensory DCDHF-hydrazone molecular switch: response to alkaline analytes. RSC Adv 6(104):102296–102305
5. Li L, Gao P, Baumgarten M, Mullen K, Lu N, Fuchs H, Chi L (2013) High performance field-effect ammonia sensors based on a structured ultrathin organic semiconductor film. Adv Mater 25(25): 3419–3425
6. Khattab TA (2018) Novel solvatochromic and halochromic sulfahydrazone molecular switch. J Mol Struct 1169:96–102
7. Abou-Yousef H, Khattab TA, Youssef YA, Al-Balakocy N, Kamel S (2017) Novel cellulose-based halochromic test strips for naked-eye detection of alkaline vapors and analytes. Talanta 170:137–145
8. Khattab TA, Gaffer HE (2016) Synthesis and application of novel tricyanofuran hydrazone dyes as sensors for detection of microbes. Color Technol 132(6):460–465
9. Thakur VK, Thakur MK (2014) Processing and characterization of natural cellulose fibers/thermoset polymer composites. Carbohydr Polym 109:102–117
10. de Oliveira Barud HG, da Silva RR, da Silva Barud H, Tercjak A, Gutierrez J, Lustri WR, de Oliveira Junior OB, Ribeiro SJL (2016) A multipurpose natural and renewable polymer in medical applications: bacterial cellulose. Carbohydr Polym 153:406–420
11. Kumar MNVR (2000) A review of chitin and chitosan applications. React Funct Polym 46(1):1–27
12. Francis Suh J-K, Matthew HWT (2000) Application of chitosan-based polysaccharide biomaterials in cartilage tissue engineering: a review. Biomaterials 21(24):2589–2598
13. Ngah WW, Teong LC, Hanafiah MAKM (2011) Adsorption of dyes and heavy metal ions by chitosan composites: a review. Carbohydr Polym 83(4):1446–1456
14. Kong M, Chen XG, Xing K, Park HJ (2010) Antimicrobial properties of chitosan and mode of action: a state of the art review. Int J Food Microbiol 144(1):51–63
15. Thakur VK, Voicu SL (2016) Recent advances in cellulose and chitosan based membranes for water purification: a concise review. Carbohydr Polym 146:148–165
16. Xu D, Qiu J, Wang Y, Yan J, Liu G-S, Yang B-R (2017) Chitosan-assisted buffer layer incorporated with hydroxypropyl methylcellulose-coated silver nanowires for paper-based sensors. Appl Phys Express 10(6):065002
17. Luo Y, Teng Z, Li Y, Wang Q (2015) Solid lipid nanoparticles for oral drug delivery: chitosan coating improves stability, controlled delivery, mucoadhesion and cellular uptake. Carbohydr Polym 122: 221–229
18. Mansur AAP, Mansur HS (2015) Quantum dot/glycol chitosan fluorescent nanoconjugates. Nanoscale Res Lett 10(1):172
19. Geng Z, Zhang H, Xiong Q, Zhang Y, Zhao H, Wang G (2015) A fluorescent chitosan hydrogel detection platform for the sensitive

and selective determination of trace mercury (II) in water. J Mater Chem A 3(38):19455–19460
20. Barata JFB, Pinto RJB, Vaz Serra VIRC, Silvestre AJD, Trindade T, Neves MGPMS, Cavaleiro JAS, Daina S, Sadocco P, Freire CSR (2016) Fluorescent bioactive corrole grafted-chitosan films. Biomacromolecules 17(4):1395–1403
21. Li Y, Liu Z, Zhu W, Fu H, Ding Y, Xie J, Yang W, Li L, Cheng C (2015) Two different emission-wavelength fluorescent probes for aluminum ion based on tunable fluorophores in aqueous media. J Fluoresc 25(3):603–611
22. Seema H, Shirinfar B, Shi G, Youn S, Ahmed N (2017) Facile synthesis of a selective biomolecule Chemosensor and fabrication of its highly fluorescent graphene complex. J Phys Chem B 121(19):5007–5016
23. Dong JX, Gao ZF, Zhang Y, Li BL, Li NB, Luo HQ (2017) A selective and sensitive optical sensor for dissolved ammonia detection via agglomeration of fluorescent ag nanoclusters and temperature gradient headspace single drop microextraction. Biosens Bioelectron 91:155–161
24. Schaude C, Meindl C, Frohlich E, Attard J, Mohr GJ (2017) Developing a sensor layer for the optical detection of amines during food spoilage. Talanta 170:481–487
25. El-Sherbiny IM, Hefnawy A, Salih E (2016) New core–shell hyperbranched chitosan-based nanoparticles as optical sensor for ammonia detection. Int J Biol Macromol 86:782–788
26. Khairy GM, Azab HA, El-Korashy SA, Steiner M-S, Duerkop A (2016) Validation of a fluorescence sensor Microtiterplate for biogenic amines in meat and cheese. J Fluoresc 26(5):1905–1916
27. Chen Y, Zhu C, Cen J, Bai Y, He W, Guo Z (2015) Ratiometric detection of pH fluctuation in mitochondria with a new fluorescein/cyanine hybrid sensor. Chem Sci 6(5):3187–3194
28. Jiao Y, Liu X, Zhou L, He H, Zhou P, Duan C, Peng X (2018) A fluorescein derivative-based fluorescent sensor for selective recognition of copper (II) ions. J Photochem Photobiol A Chem 355:67–71
29. Bao X, Cao Q, Wu X, Shu H, Zhou B, Geng Y, Zhu J (2016) Design and synthesis of a new selective fluorescent chemical sensor for Cu2+ based on a pyrrole moiety and a fluorescein conjugate. Tetrahedron Lett 57(8):942–948
30. Warratz R (2016) Electrochemical gas sensor with an ionic liquid as electrolyte for the detection of ammonia and amines. US Patent 9:395,323
31. Mirmohseni A, Oladegaragoze A (2003) Construction of a sensor for determination of ammonia and aliphatic amines using polyvinylpyrrolidone coated quartz crystal microbalance. Sensors Actuators B Chem 89(1–2):164–172
32. Crowley K, Morrin A, Hernandez A, O'Malley E, Whitten PG, Wallace GG, Smyth MR, Killard AJ (2008) Fabrication of an ammonia gas sensor using inkjet-printed polyaniline nanoparticles. Talanta 77(2):710–717
33. Hanson DR, McMurry PH, Jiang J, Tanner D, Huey LG (2011) Ambient pressure proton transfer mass spectrometry: detection of amines and ammonia. Environ Sci Technol 45(20):8881–8888
34. Diaz YJ, Page ZA, Knight AS, Treat NJ, Hemmer JR, Hawker CJ, de Alaniz JR (2017) A versatile and highly selective colorimetric sensor for the detection of amines. Chem Eur J 23(15):3562–3566
35. Huang X, Hu N, Gao R, Yu Y, Wang Y, Yang Z, Kong ESW, Wei H, Zhang Y (2012) Reduced graphene oxide-polyaniline hybrid: preparation, characterization and its applications for ammonia gas sensing. J Mater Chem 22(42):22488–22495
36. Takagai Y, Nojiri Y, Takase T, Hinze WL, Butsugan M, Igarashi S (2010) "Turn-on" fluorescent polymeric microparticle sensors for the determination of ammonia and amines in the vapor state. Analyst 135(6):1417–1425
37. Saharan V, Sharma G, Yadav M, Choudhary MK, Sharma SS, Pal A, Raliya R, Biswas P (2015) Synthesis and in vitro antifungal efficacy of cu–chitosan nanoparticles against pathogenic fungi of tomato. Int J Biol Macromol 75:346–353
38. Deng X, Cao M, Zhang J, Hu K, Yin Z, Zhou Z, Xiao X, Yang Y, Sheng W, Wu Y, Zeng Y (2014) Hyaluronic acid-chitosan nanoparticles for co-delivery of MiR-34a and doxorubicin in therapy against triple negative breast cancer. Biomaterials 35(14):4333–4344
39. Armarego WLF, Chai CLL (2013) Purification of laboratory chemicals. Butterworth-Heinemann
40. Lide DR (2004) CRC handbook of chemistry and physics 2004–2005: a ready-reference book of chemical and physical data
41. March J (1992) Advanced organic chemistry: reactions, mechanisms, and structure. John Wiley & Sons
42. Albert A (2012) The determination of ionization constants: a laboratory manual. Springer Science & Business Media
43. Perrin DD (1972) Dissociation constants of organic bases in aqueous solution: supplement 1972. Butterworths
44. Widmer S, Dorrestijn M, Camerlo A, Urek SK, Lobnik A, Housecroft CE, Constable EC, Scherer LJ (2014) Coumarin meets fluorescein: a Förster resonance energy transfer enhanced optical ammonia gas sensor. Analyst 139(17):4335–4342
45. Preininger C, Ludwig M, Mohr GJ (1998) Effect of the sol-gel matrix on the performance of ammonia fluorosensors based on energy transfer. J Fluoresc 8(3):199–205
46. Cao L-W, Wang H, Li J-S, Zhang H-S (2005) 6-oxy-(N-succinimidyl acetate)-9-(2′-methoxycarbonyl) fluorescein as a new fluorescent labeling reagent for aliphatic amines in environmental and food samples using high-performance liquid chromatography. J Chromatogr A 1063(1–2):143–151
47. Cao L, Wang H, Ma M, Zhang H (2006) Determination of biogenic amines in HeLa cell lysate by 6-oxy-(N-succinimidyl acetate)-9-(2′–methoxycarbonyl) fluorescein and micellar electrokinetic capillary chromatography with laser-induced fluorescence detection. Electrophoresis 27(4):827–836